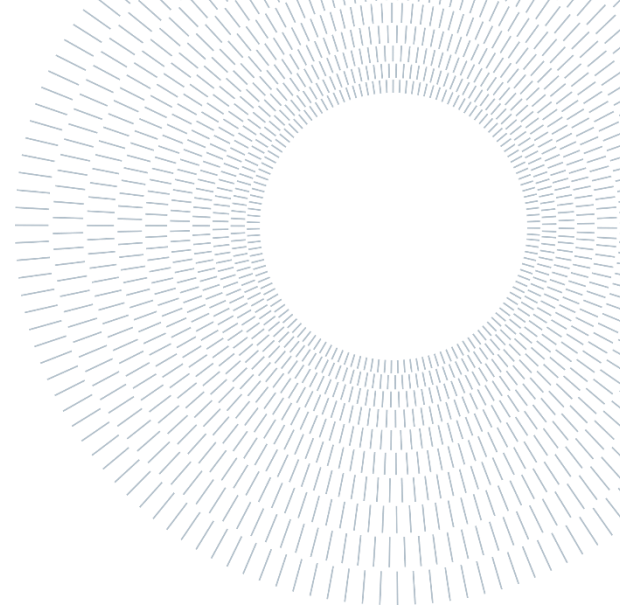




POLITECNICO
MILANO 1863

SCUOLA DI INGEGNERIA INDUSTRIALE
E DELL'INFORMAZIONE



EXECUTIVE SUMMARY OF THE THESIS

Modelling atrial and ventricular hiPSC cardiomyocytes microtissues within a 3D beating organ on a chip: a mechanical, electrical and biological study

TESI MAGISTRALE IN BIOMEDICAL ENGINEERING – INGEGNERIA BIOMEDICA

AUTHOR: Andrea Enrico Bortolotti

ADVISOR: Paola Occhetta

ACADEMIC YEAR: 2023-2024

1. Introduction

The heart is a hollow muscular organ, located near the anterior wall of the chest, just behind the breastbone, and its role is to collect deoxygenated blood from the body periphery and pump it back in the body before getting re-oxygenated by passing through the lungs [1]. The ability to generate force to push the blood through the cardiovascular system is up to its composition. The cardiac wall is composed by three layers, the pericardium, which is the outer one, the myocardium, which is middle one, and the endocardium, which is the inner one [2]. The heart from a macroscopic point of view, is divided into four chambers, two atria and two ventricles and between them there are four valves allowing the unidirectional blood flow avoiding backflow [1]. Meanwhile, from a microscopic point of view, the heart is a highly organized complex tissues made by different kind of cells such as cardiomyocytes, cardiac fibroblasts, conduction cells, cardiac stem cells and endothelial cells [2]. Electrical and mechanical activity of atrial and ventricular

microtissues are made possible to the presence of connection between cardiomyocytes [3]. This connection, called junction, are the adherens, desmosomal and gap junction and allow the propagation of the electrical signal [4]. Atria and ventricles possess different mechanical and electrical properties [3]. Electrically the differences lie on the action potential in each of its phase:

- Phase 0: Atrial cells have a more hyperpolarized resting potential compared to ventricular cells, leading to a lower threshold for depolarization and activation of fast-activating sodium channels.
- Phase 1: Atrial cells have shorter and less intense action potentials compared to ventricular cells due to the larger amplitude of the transient outward current (I_{to}), leading to a quicker repolarization.
- Phase 2: Atrial cells have a shorter phase 2 duration compared to ventricular cells due to the dominance of the ultrarapid delayed rectifier current (I_{Kur}) in atrial cells, leading to faster repolarization.

- Phase 3: Both atrial and ventricular cells rely on delayed rectifier potassium currents (IK) for repolarization, but the timing and balance of these currents may differ between the cell types.
- Phase 4: Ventricular cells have a slightly more negative resting membrane potential compared to atrial cells due to a higher level of inward rectifier expression. (Figure 1.1).

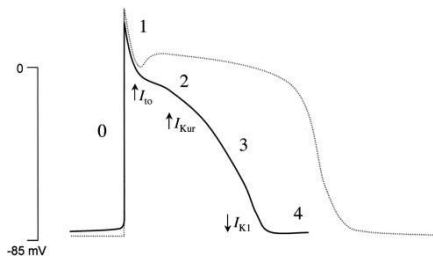


Figure 1.1: Comparison between ventricular action potential (dotted line) and atrial action potential (solid line). Ventricular action potential exhibits a less negative resting potential, a shortened plateau phase, and a slower terminal repolarization respect atrial one. Take from [5]

From a mechanical point of view, the contractile properties are different among atrial and ventricular cardiomyocytes because of their protein composition. Myosin is the central molecular motor of the heart, which composes the cross-bridge cycling and regulates both ATP hydrolysis and mechanical production of contractile force. Myosin presents two heavy chains isoforms, α and β , and two light chains with two isoforms, MLC-2a specific for atrial cardiomyocytes and MLC-2v for ventricular cardiomyocytes [3]. Atrial myocardium is recognized for its higher maximum shortening velocity (V_{max}) compared to ventricular myocardium. The rate of active tension generation and relaxation in atrial myofibrils is also quicker than in ventricular myofibrils, which is thought to be due to differences in cross-bridge kinetics. Furthermore, the atrial working myocardium not only has a higher shortening rate but also produces less active tension compared to the ventricular myocardium. This difference in maximum tension development between the atrium and ventricle may be due to variations in the expression of myosin light chain (MLC) isoforms, which can influence aspects of cross-bridge cycling and force development [3].

Cardiovascular diseases are a leading cause of death globally, accounting for around 30% of all deaths. These diseases involve dysfunction in the vascular, cardiac, and nervous systems. There is a need for innovative medications and treatments to reduce the global burden of CVDs. Currently, heart disease is primarily treated through transplantation due to the limited effectiveness of drugs in slowing down the disease progression. The process of drug development is expensive and time-consuming, making screening testing crucial for improving the efficiency of drug development. In vitro solutions, in accordance with the 3Rs (Replacement, Reduction and Refinement) are needed to address ethical issues in drug testing. In recent years, in vitro techniques such as 2D and 3D cell cultures have been developed to mimic heart physiology as preclinical model to support drug development (i.e. both to test efficacy of CVDs drug, or more in general to test the cardiotoxicity of any new molecule), but these models lack physiological relevance. The emergence of heart on a chip models, which combine 3D structured microarchitectures with mechanical or electrical stimulations, offers a more physiologically relevant setup for drug screening testing. This models have the potential to enhance cell maturation and provide more consistent outcomes in drug development [6]. One major drawback of the current organ-on-a-chip model is the lack of both electrical recording and stimulation capabilities, as well as challenges in production. This thesis aims to characterize mechanically, electrically and biologically hiPSC atrial and ventricular microtissues on a 3D beating organ on a chip to establish a benchmark for future drug screening test. To this aim, the platform used for this project is uStretch (Biomimx s.r.l.), which is able to overcome several limitations of current heart-on-a-chip [7] enabling easy production and allowing for both electrical recording and stimulation. Lacking the existence of a heart on a chip model able to allow the co-culture of atrial and ventricular microtissues, the final aim of the thesis is to propose a new microfluidic device able to study simultaneously atrial and ventricular microtissues to have a more complete representation of the heart complex architecture.

2. Materials and methods

Microfluidic platform

The microfluidic device utilized in this study is the uStretch platform (BiomimX® S.r.l.). This chip is composed by three layers: a PDMS top layer, a PDMS actuation layer and a glass coverslip. The top layer includes three cell culture chambers equipped with central channels and hanging pillars for supporting 3D cell-laden fibrin gel. Additionally, there are two side medium channels for delivering cell culture medium. (Figure 2.1).



Figure 2.1: uStretch® platform produced by BiomimX® S.r.l

Each chamber in the chip has two holes for injection, one inlet and one outlet, with a 1mm diameter. There are also four reservoirs for medium replacement in each chamber, connected to medium channels with a 5mm diameter. The central channel is 300 μm wide, 10 mm long, and 150 μm high, with a 40 μm gap between pillars. The actuation layer is 800 μm thick and can be pressurized to mechanically stimulate the microtissues. There are four electrode channel guides, two for each side, and one allows the insertion of electrode in the cell chamber for electrical recording and the other allows the insertion of electrode in the medium channel for the electrical stimulation (Figure 2.2).

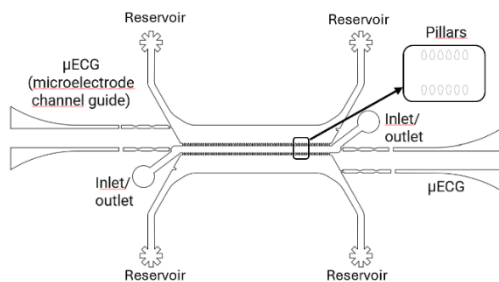


Figure 2.2: microfluidic one chamber CAD design of one top layer with a focus on the pillars shape.

The chip is produced by replica molding process. To obtain them, PDMS (Sylicard 184 Silicon Elastomer Kit) was mixed in a 1:10 ratio of curing agent to pre-polymer and poured into acrylic resin molds (10 10 CFS, C-system) to create the culture layer (top layer). The same process was used on a micropatterned wafer for the actuation layer in order to have an 800 μm thickness. For uStretch platforms, the two layers were bonded together using plasma treatment (Harrick Plasma, PDC-002). Afterwards the two layers bonded together are punched in the actuation hole with a 1.5mm puncher. In the end the two layers have bonded with the glass coverslip.

Cell source and injection

After following thawing and culturing protocols for human cardiac fibroblasts, hi-PSC atrial cardiomyocytes and hi-PSC ventricular cardiomyocytes (Axol Bioscience), the injection was performed. Firstly, human cardiac fibroblasts were thawed and cultured with their specific medium until they reached confluency in order to have an average of one million human cardiac fibroblasts per experiment. Afterwards, atrial and ventricular cardiomyocytes were thawed and the injection was performed.

Cardiac microtissues, both atrial and ventricular, are composed by 75% of cardiomyocytes and 25% of cardiac fibroblasts, moreover the final cell density must be in the range between 85×10^6 - 125×10^6 cells/ml in a final fibrin gel composed by 10 mg/ml of fibrinogen and 2.5U/ml of thrombin. After the injection day, the mechanical stimulation was applied from the second day till the last of the experiment, which was day 11 in our experiments. After day 11 the chips were fixed to be conserved for immunostaining analysis.

Mechanical readout

Video recording of beating cardiac microtissues was conducted using a microscope with 10X magnification at a frame rate of 20 frames per second for 60 seconds. The analysis of the video was performed using MuscleMotion, an ImageJ® plugin, which allows for quantitative analysis of the microtissue contractions [8]. The program extracts key parameters such as contraction amplitude, time to peak, relaxation time, and beating period based on pixel variations between

frames. For each microtissues were taken two different videos and only the best of them was used for measurement. The video recording of microtissues on days 5, 6, 7, 8, and 11 of culturing was divided into three Regions of Interest (ROIs) for analysis. MuscleMotion software calculated parameters of interest for each ROI, with results averaged for each ROI (Figure 2.3). Pearson's correlation coefficient was calculated from the normalized contraction trend to evaluate mechanical stimulation effects on microtissue pulse, comparing dynamic and static microtissues. Data was analyzed across days to identify the most optimal day based on correlation coefficient, contraction amplitude, beating period, relaxation time and time to peak.

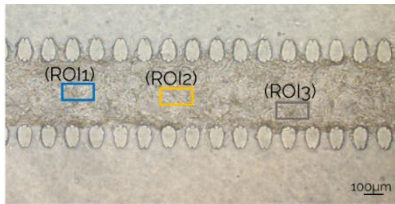


Figure 2.3: three ROIs taken from one microtissue for MuscleMotion analysis

Electrical readout

To compare the electrical behavior of atrial and ventricular microtissues, field potential recordings were taken on day 11. The acquisition system used in the study consists of five main components including recording electrode, reference electrode, pre-amplifier, extracellular amplifier, and electronic board. The recording electrode, made of stainless-steel microneedle, is inserted into the μ Stretch through the μ ECG recording line. An AgCl ground electrode is placed in the cell culture medium reservoir opposite to the recording electrode (Figure 2.4).

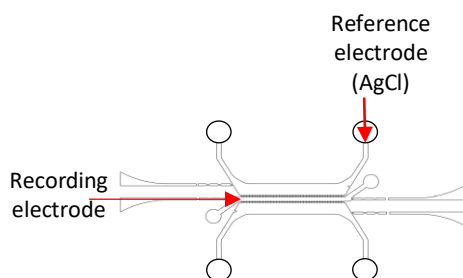


Figure 2.4: schematic representation about the electric set-up acquisition system.

During the experiment, the μ Stretch was kept in an incubator at 37°C with 5% CO₂, and the electrodes were linked to an extracellular amplifier (Ext-02b, Npi Electronic GmbH, Germany) set at a gain of 1×10^4 and a bandpass filter from 0.3 Hz to 10 kHz. The field potentials of the atrial and ventricular microtissues were recorded using an electronic board (Analog Discovery 2, Digilent, Washington) at a sampling rate of 2000 samples per second [9]. Three main parameters were derived from each signal: spike amplitude, beating period (the time between two depolarization peaks), and field potential duration (the time between the depolarization and repolarization peaks) (Figure 2.5).

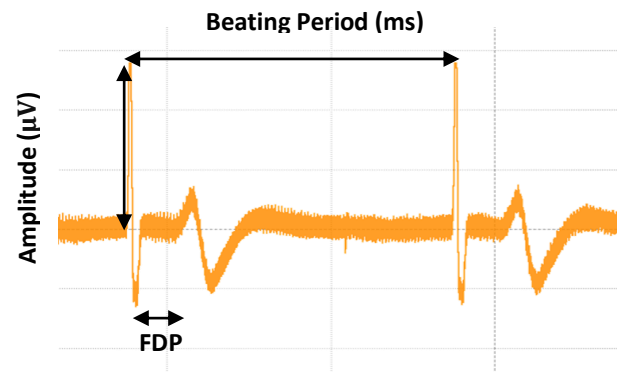


Figure 2.5: recorded ECG signal showing the three parameters of interest, which are the beating period, spike amplitude and field potential duration.

Biological readout

Immunofluorescence analysis was conducted on fixed microdevices using a specific protocol. After removing the medium, the chambers were washed with PBS (Invitrogen, D1306). Following this, paraformaldehyde (PFA) 4% (Merck, 158127) was added and the device was incubated at room temperature for 20 minutes before being washed with PBS. The chip was then inverted, placed in a Petri dish, covered with PBS, sealed with parafilm, and stored in the refrigerator at 4°C until the day of immunostaining. In order to assess the organization of atrial and ventricular microtissues, specific antibodies were selected [10]: cardiac troponin I (rabbit, IgG2a, SantaCruz, 1:100), vimentin (chicken, IgY, Abcam 1:1000), DAPI for nucleus staining (1:100), myosin light chain-2

ventricular (rabbit, IgG, Abcam, 1:150), and sarcolipin (rabbit, IgG, Thermofisher, 1:100). The immunofluorescence sample was washed twice with PBS for 10 minutes each wash. A solution containing 0.1% Tween-20 20 (Sigma Aldrich, 038K00914), 2% BSA (w/v), and PBS was applied to the wells in 150 μ l increments and left to incubate at room temperature for 1 hour. Tween-20 facilitates the permeabilization of cell membranes for staining cytoskeletal proteins, while BSA helps prevent non-specific binding. Following this step, the blocking solution was substituted with a 200 μ l primary antibody solution, tailored to the specific dilution of each antibody and supplemented with 0.5% Goat serum (Sigma Aldrich, SLCK7210) for each microtissue in the 4 wells. The microtissues were then refrigerated overnight at 4°C.

Once the primary antibody solution was removed, the micro-constructs underwent two washes with PBS, each separated by a 20-minute interval. Subsequently, secondary antibodies including Alexa Fluor 488 Goat anti-mouse (Invitrogen, A-11008), Alexa Fluor 488 Goat anti-chicken (Invitrogen, A-11008), Alexa Fluor 546 goat anti-mouse (Invitrogen, A-11030), and Alexa Fluor 546 goat anti-rabbit (Invitrogen, A-11030) were applied and allowed to incubate at room temperature for 2 hours. The solution was then replaced with a 300 nM DAPI working solution in PBS, which was added to the devices and incubated overnight at 4°C in darkness to stain cell nuclei for identification purposes.

Statistical analysis

The mean values for beating period, Person's correlation coefficient, contraction amplitude, time to peak, and time to relaxation were calculated for each sample of static and dynamic atrial and ventricular microtissues. Subsequently, the data was segregated based on static and dynamic conditions to investigate the impact of mechanical stimulation on cell development and beating characteristics. Statistical analyses were conducted using GraphPad Prism 9 software, with normal distribution of datasets evaluated using One Way Anova with Tukey's multiple comparison test across all days of data collection. Significance levels were indicated as * $p < 0.05$, ** $p < 0.01$, *** $p < 0.001$, and **** $p < 0.0001$, and the results were reported as mean \pm SD.

3. Results

Mechanical results

The initial comparison involves analyzing the mechanical stimulation effect on atrial and ventricular samples, comparing static and dynamic conditions. Pearson's correlation coefficient was used for this comparison. The data from the graphs indicate a significant difference in the correlation coefficient, particularly on day 5. For atrial samples on day 5, the mean under static conditions is 0.0451847667 with a standard deviation of ± 0.029757 , whereas the mean under dynamic conditions is 0.6062896478 with a standard deviation of ± 0.238296 . Similarly, ventricular samples on day 5 show a mean of 0.270748 and a standard deviation of ± 0.069574 under static conditions, and a mean of 0.9435566 and a standard deviation of ± 0.058113 under dynamic conditions. The dynamic samples consistently exhibit a higher correlation coefficient compared to the static samples, although this difference decreases over time (Figure 3.1).

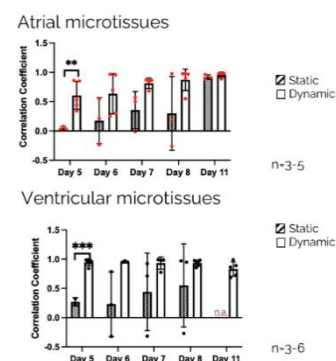


Figure 3.1: comparison between dynamic and static condition for both atrial (red dots) and ventricular (black dots) microtissues. Statistical test performed to obtain statistical significance (** $P < 0.01$ and *** $P < 0.001$).

Comparison of dynamic samples shows that ventricular microtissues generally have more synchronized beating than atrial microtissues, except on day 11 when the atrial samples showed a higher Pearson's correlation coefficient (0.9563 ± 0.04641) compared to the ventricular samples (0.83 ± 0.1238). The trend is consistent in static conditions as well, but the high standard deviation in the results makes them statistically insignificant (Figure 3.2).

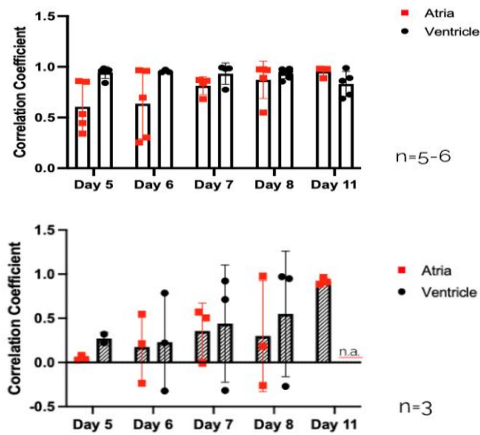


Figure 3.2: the upper histogram is about the correlation coefficient comparison between dynamic samples and the bottom one is about the correlation coefficient between static ones.

Following an understanding of the mechanical stimulation efforts, each MuscleMotion parameter was analyzed (Figure 3.3). In terms of atrial dynamic microtissues, the beating period remained consistent over time, starting at an average of 2176.76 ms with a standard deviation of ± 506.557 ms on day 5, and decreasing to 2066.941 ms with a standard deviation of ± 556.7486 ms. The contraction amplitude increased as time progressed, with an initial value of 35.17427 a.u. ± 12.44349 on day 5, reaching a peak of 149.9467 a.u. ± 40.63089 on day 8. The time to peak slightly decreased from an average of 694.5876 ms ± 508.9706 ms on day 5 to 532.8836 ms ± 155.1602 ms on day 11. Similarly, the relaxation time slightly increased from an average of 651.2254 ms ± 289.2517 ms on day 5 to 795.436 ms ± 129.0878 ms on day 11. On the other hand, for ventricular microtissues, the beating period slightly decreased over time, starting at an average of 2475.125 ms with a standard deviation of ± 717.9613 ms on day 5, and decreasing to 1510.365 ms with a standard deviation of ± 453.87 ms. The contraction

amplitude increased over time, starting at 37.30596 a.u. ± 19.89733 on day 5 and peaking at 82.62861 a.u. ± 11.29409 on day 7. The time to peak slightly decreased from an average of 645.7756 ms ± 111.4107 ms on day 5 to 585.6717 ms ± 264.0015 ms on day 11. Similarly, the time to relaxation also slightly decreased from an average of 623.3852 ms ± 188.8935 ms on day 5 to 465.8487 ms ± 145.6313 ms on day 11.

The amplitude of contractions in atrial samples shows a slight increase in the first three days, but this discrepancy becomes statistically significant in the final two days. Specifically, atrial samples exhibit an amplitude of 149.94 ± 40.63 a.u. on day 8 and 142.055 ± 20.65 a.u. on day 11, whereas ventricular samples have an amplitude of 56.81 ± 33.80 on day 8 and 59.15 ± 21.17 on day 11.

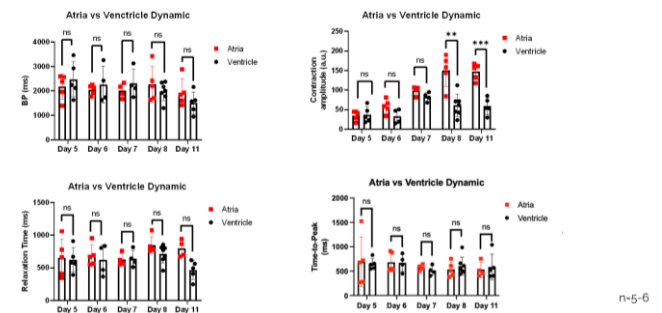


Figure 3.3: graphs showing beating period, contraction amplitude, time to peak and relaxation time for atrial dynamic microtissues (red dots), from day 5 to day 11 of culturing, and ventricular dynamic microtissues (black dots). Statistical test performed to obtain statistical significance (**** $P < 0.0001$, *** $P < 0.001$, ** $P < 0.01$ and * $P < 0.05$).

Electrical results

The protocol for electrical characterization has been followed, with the goal of studying the electrophysiological characteristics of atrial and ventricular microtissues.

The examination of four field potential parameters in the atrium and ventricle demonstrated clear differences in their characteristics. Specifically, the analysis revealed that atrial samples (red dots) had an average spike amplitude of 293.33 μV with a narrow standard deviation of ± 9.8657 μV , whereas ventricular samples (black dots) had a lower average spike amplitude of 154.25 μV with a larger standard deviation of ± 92.13 μV (Figure 3.4).

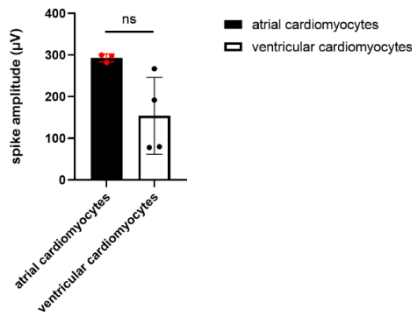


Figure 3.4: spike amplitude comparison between atrial and ventricular samples at day 11 of culturing. Statistical test performed to obtain statistical significance (ns with $P>0.05$).

In terms of the other three parameters, atrial cardiomyocytes have a mean beating period of $1074.667 \text{ ms} \pm 42.194 \text{ ms}$, while ventricular cardiomyocytes have a mean beating period of $1120 \text{ ms} \pm 668.691 \text{ ms}$. The field potential duration (FDP) is $216.333 \text{ ms} \pm 46.45 \text{ ms}$ for atrial samples and $309.75 \text{ ms} \pm 81.79 \text{ ms}$ for ventricular samples. When Fridericia's correction is applied, the FDP is $212.33 \text{ ms} \pm 44.07 \text{ ms}$ for atrial samples and $305 \text{ ms} \pm 55.19 \text{ ms}$ for ventricular samples (Figure 3.5).

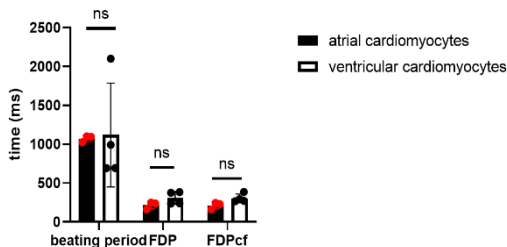


Figure 3.5: beating period, field potential duration and field potential duration after Fridericia's correction comparison between atrial and ventricular samples after 11 day of culturing. Statistical test performed to obtain statistical significance (ns with $P>0.05$).

Biological results

During the biological characterization, a review of the literature was conducted to identify specific markers for atrial and ventricular dynamic samples used in immunostaining studies. Cardiac troponin I (cTn1), ventricular myosin light chain-2 (MLC2v), sarcolipin (SLN) and vimentin (VTN)

were used to stain both atrial and ventricular samples.

The ventricular samples exhibited the expression of cardiac troponin I and vimentin, known markers of cardiac fibroblasts, as well as ventricular myosin light chain-2, which is specific to the ventricles (Figure 3.6 and 3.7) [10]. Moreover, sarcolipin, typically found in atrial tissue, was not expressed in the ventricular samples. In contrast, the atrial samples showed expression of cardiac troponin I, vimentin, and sarcolipin, confirming their atrial specificity (Figure 3.8) [10]. Furthermore, myosin light chain-2, a ventricular-specific marker, was not detected in the atrial samples.

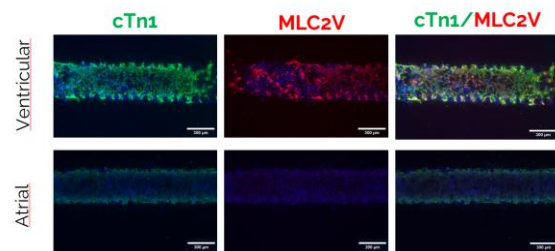


Figure 3.6: representative images of atrial (last three images) and ventricular (first three images) microtissues after 11 days of culturing in 3D in gel fibrin. Cardiac fibroblasts are identified by cardiac troponin I (green), ventricular cardiomyocytes by ventricular myosin light chain 2 (red) and atrial cardiomyocytes are not stained because they don't express myosin light chain ventricular being a specific ventricular marker. Nuclei are stained with DAPI (blue).

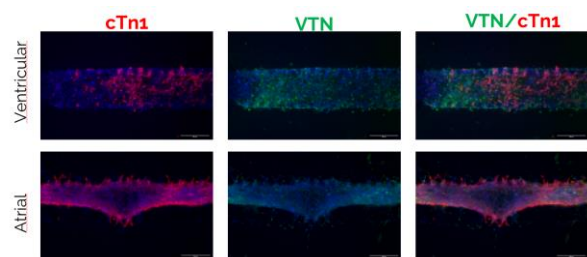


Figure 3.7: representative images of atrial (last three images) and ventricular (first three images) microtissues after 11 days of culturing in 3D in gel fibrin. Cardiac fibroblasts are identified by cardiac troponin I (red) and vimentin (green). Nuclei are stained with DAPI (blue).

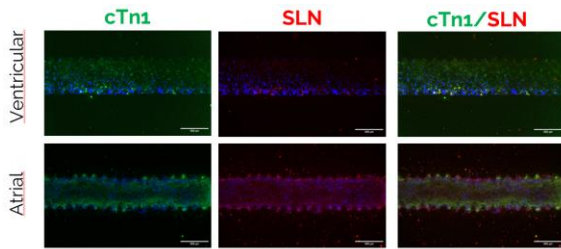


Figure 3.8: representative images of atrial (last three images) and ventricular (first three images) microtissues after 11 days of culturing in 3D in gel fibrin. Cardiac fibroblasts are identified by cardiac troponin I (green), atrial cardiomyocytes by sarcolipin (red) and ventricular cardiomyocytes are not stained because they don't express sarcolipin being a specific atrial marker. Nuclei are stained with DAPI (blue).

4. Discussion

Cardiovascular diseases are a leading cause of death globally, accounting for 30% of fatalities. Current treatment options mainly involve medications that slow down disease progression, with heart transplantation being the most effective but facing challenges like donor shortages.

To improve drug development for CVD, heart-on-a-chip models have emerged as an innovative way to recreate in vivo-like environments for drug screening testing, leading to more consistent outcomes in treatment.

This research analyzed hiPSC atrial and ventricular microtissues on a 3D beating organ chip in a comprehensive manner, focusing on mechanical, electrical, and biological characteristics to lay the groundwork for future drug screening efforts. The study uncovered significant differences between atrial and ventricular cardiomyocytes from various angles. Initially, the microtissues were observed under both static and dynamic conditions, with dynamic conditions consistently yielding superior results. The dynamic microtissues displayed stronger and more linear behavior, as evidenced by a higher Pearson's correlation coefficient and greater contraction amplitudes. The increase in contraction amplitude from static to dynamic conditions aligns with existing research, as mechanical stimulation has been shown to enhance cell alignment, contractility, and electrical conductivity [6]. This correlation coefficient behavior was in line with findings from a previous Mimic Lab project.

When studying dynamic conditions, atrial microtissues consistently showed an increasing

contraction amplitude over time, while ventricular microtissues displayed a slight decrease in beating period but an increase in contraction amplitude. Ventricular microtissues also exhibited a more synchronized beating pattern compared to atrial microtissues except for the final day where the trend is inverted, which doesn't contradict the expected rhythmical beating of atrial tissue compared to ventricular tissue [11]. The higher contraction amplitude in atrial microtissues towards the later days of the study was unexpected, as previous research suggested ventricular microtissues should have greater strength due to myosin light chain isoform [12].

Furthermore, while the overall mean beating period was higher for ventricular microtissues over several days, the time to peak was consistently lower for atrial microtissues on days 8 and 11. Atrial dynamic microtissues also showed longer relaxation times compared to ventricular microtissues in the later days of the study, contrary to the expected faster shortening velocity and relaxation of atrial cardiomyocytes compared to ventricular ones [3], [12].

In terms of electrical activity, atrial cardiomyocytes displayed greater spike amplitudes, quicker beating rhythms, and shorter field potential durations compared to ventricular cardiomyocytes. The lower standard deviations in these parameters for atrial samples suggested more uniform electrical activity in atrial cardiomyocytes. The spike amplitude findings contradicted previous literature, possibly due to the lower myofibril density in atrial cardiomyocytes compared to ventricular ones. On the other hand, the other results are linear with literature analysis for atrial faster shortening velocity [3], [12].

Biologically, atrial microtissues exhibited high levels of sarcolipin and did not express ventricular myosin light chain-2, while ventricular microtissues showed the opposite pattern. This expression of proteins aligned with previous literature [10].

5. Conclusions

This study is a crucial step in understanding the differences in behavior between atrial and ventricular cells in a 3D heart on a chip, setting a foundation for drug screening testing.

To fully understand the biological variances between these two types of cardiomyocytes, PCR analysis will be conducted to compare gene expression levels of calcium, sodium, and potassium channels, following initial immunostaining. This will offer insight into how gene expression variations may impact differences in action potential shape, as noted in previous research. Drug screening tests will be then carried out on day 8, when both types of microtissues reach their peak activity, to assess how treatments regulate the electrical and mechanical behavior of cardiomyocytes. Current microfluidic devices, including the one used in this study, only allow for the study of one cell type at a time, limiting a comprehensive understanding of the heart's architecture. To overcome this limitation, the project's last goal is to develop a new microfluidic chip design enabling the co-culture of atrial and ventricular cardiomyocytes to better mimic the heart's structure. The innovative approach of simultaneously studying both cell types will enhance our understanding of their interactions and improve drug screening accuracy. To this aim, a new chip layout was proposed (Figure 5.1), featuring five channels: two medium channels on the sides, and three channels in the center made up of atrial and ventricular channels separated by a channel composed of endothelial cells and collagen. This layer is designed to replicate the architecture of the endocardium that surrounds the heart's valves, separating the atrium from the ventricle. By incorporating this feature into the current model, we could create a more accurate representation of the heart's structure.

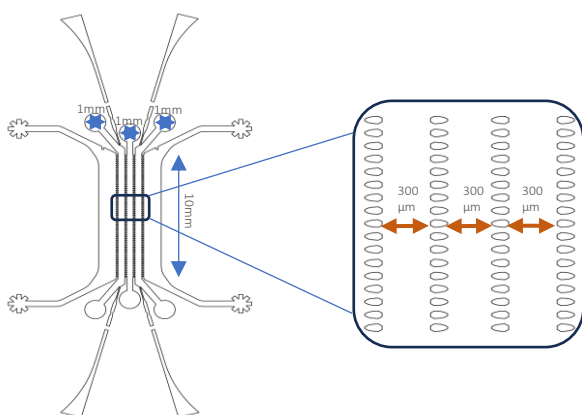


Figure 5.1: CAD design of a new microfluidic device which allows the co-culture of both atrial and ventricular microtissues on the extreme channels while in the middle one is reserved to a microtissue made by endothelial cells and collagen.

6. Bibliography

- [1] A. J. Weinhaus e K. P. Roberts, «Anatomy of the Human Heart», in *Handbook of Cardiac Anatomy, Physiology, and Devices*, P. A. Iaizzo, A. c. di, Totowa, NJ: Humana Press, 2005, pp. 51–79. doi: 10.1007/978-1-59259-835-9_4.
- [2] S. Shah, G. Gnanasegaran, J. Sundberg-Cohon, e J. Buscombe, «The Heart: Anatomy, Physiology and Exercise Physiology», in *Integrating Cardiology for Nuclear Medicine Physicians: A Guide to Nuclear Medicine Physicians*, 2009, pp. 3–22. doi: 10.1007/978-3-540-78674-0_1.
- [3] S. Y. Ng, C. K. Wong, e S. Y. Tsang, «Differential gene expressions in atrial and ventricular myocytes: insights into the road of applying embryonic stem cell-derived cardiomyocytes for future therapies», *Am. J. Physiol.-Cell Physiol.*, vol. 299, fasc. 6, pp. C1234–C1249, dic. 2010, doi: 10.1152/ajpcell.00402.2009.
- [4] W. Dun e P. A. Boyden, «The Purkinje cell; 2008 style», *J. Mol. Cell. Cardiol.*, vol. 45, fasc. 5, pp. 617–624, nov. 2008, doi: 10.1016/j.yjmcc.2008.08.001.
- [5] D. Fatkin, R. Otway, e J. Vandenberg, «Genes and Atrial Fibrillation A New Look at an Old Problem», *Circulation*, vol. 116, pp. 782–92, set. 2007, doi: 10.1161/CIRCULATIONAHA.106.688889.
- [6] B. Gu *et al.*, «Heart-on-a-chip systems with tissue-specific functionalities for physiological, pathological, and pharmacological studies», *Mater. Today Bio*, vol. 24, p. 100914, feb. 2024, doi: 10.1016/j.mtbio.2023.100914.
- [7] A. Marsano *et al.*, «Beating heart on a chip: a novel microfluidic platform to generate functional 3D cardiac microtissues», *Lab. Chip*, vol. 16, fasc. 3, pp. 599–610, gen. 2016, doi: 10.1039/C5LC01356A.
- [8] L. Sala *et al.*, «MUSCLEMOTION», *Circ. Res.*, vol. 122, fasc. 3, pp. e5–e16, feb. 2018, doi: 10.1161/CIRCRESAHA.117.312067.
- [9] R. Visone *et al.*, «Predicting human cardiac QT alterations and pro-arrhythmic effects of compounds with a 3D beating heart-on-chip platform», *Toxicol. Sci.*, vol. 191, fasc. 1, pp. 47–60, ott. 2022, doi: 10.1093/toxsci/kfac108.

- [10] I. Goldfracht *et al.*, «Generating ring-shaped engineered heart tissues from ventricular and atrial human pluripotent stem cell-derived cardiomyocytes», *Nat. Commun.*, vol. 11, p. 75, gen. 2020, doi: 10.1038/s41467-019-13868-x.
- [11] S. K. Padala, J.-A. Cabrera, e K. A. Ellenbogen, «Anatomy of the cardiac conduction system», *Pacing Clin. Electrophysiol. PACE*, vol. 44, fasc. 1, pp. 15–25, gen. 2021, doi: 10.1111/pace.14107.
- [12] H. Yamashita *et al.*, «Myosin light chain isoforms modify force-generating ability of cardiac myosin by changing the kinetics of actin-myosin interaction», *Cardiovasc. Res.*, vol. 60, fasc. 3, pp. 580–588, dic. 2003, doi: 10.1016/j.cardiores.2003.09.011.